A Gated Recurrent Units Based Particle Filter for Unmanned Underwater Vehicle State Estimation

Changjian Lin, Hongjian Wang, *Member, IEEE*, Mingyu Fu, Jianya Yuan, and Jason Gu, *Member, IEEE*

***Abstract*—Target state estimation is a key technology for unmanned underwater vehicles to achieve target tracking, collision avoiding, formation control, and other tasks. Compared with other measurement methods, underwater measurement has lower reliability due to the uncertainty of sonar detection. In this case, the performance of target state estimation depends heavily on the target motion model. However, the dynamics of unmanned underwater vehicles are very complex and nonlinear. Although many state estimation methods for nonlinear systems have been proposed, the complex dynamics of unmanned underwater vehicle and uncertainty in sonar detection remain challenges for underwater target state estimation problems. This paper proposes a gated recurrent units-based particle filter to improve the performance of the target state estimator for unmanned underwater vehicles. A deep neural network framework based on gated recurrent units is used to establish the mapping between the previous measurements and the current target states. This neural network learns the dynamics model of unmanned underwater vehicles and recognizes the measurement noise. The proposed filter samples from previous measurements of the target unmanned underwater vehicle, and the fully trained deep neural network predicts the current states of the sampled particles. The proposed method solves the low accuracy and instability caused by motion modeling errors and system nonlinearity. Simulation results show that the proposed gated recurrent units-based particle filter for unmanned underwater vehicle state estimation has better accuracy and stability than the traditional state estimation methods. All simulations are done with the noise which is Gaussian noise pass through a nonlinear transformation.**

***Index Terms*—Deep neural networks, gated recurrent units, particle filter, target state estimation, and unmanned underwater vehicle.**

I. Introduction

TARGET tracking is a basic technology that supports unmanned underwater vehicles (UUVs) to perform a variety of tasks. UUV target state estimation is the core technology of UUV target tracking, and its estimation accuracy affects the performance of target tracking directly. Accurate location and motion estimation of UUV is essential in both commercial and military fields [1]. Target state estimation refers to obtaining the predicted target states through some known target prior knowledge. And the measured information of target states obtained by sensors is used to modify the previous target states through a certain algorithm. Although underwater target state estimation has made significant progress in recent years [2-8], it is still a difficult task to develop a powerful target state estimation algorithm to achieve high-precision UUV state estimation based on sonar detection.

At present, the state estimation methods used to solve the target tracking problem mainly include Kalman Filter (KF) [9], Extended Kalman Filter (EKF) [10, 11], Unscented Kalman Filter (UKF) [12-14], and particle filter (PF) [15-17]. EKF is simple and easy to implement, but it needs to calculate the nonlinear function Jacobian matrix. Although UKF does not need to calculate nonlinear Jacobian matrix, the convergence effect depends too much on the selection of parameters in the algorithm that are complex. PF can solve the problem of state estimation of non-linear non-gaussian system, and if the number of particles is enough, the error of particle filter can be deduced to converge to zero in theory.

In order to overcome the above shortcomings of conventional filters and improve the accuracy of filtering, researchers have made many contributions. To solve the problems of low precision and poor stability of KF in nonlinear and non-Gaussian environments, Ito [18] proposed a central difference filter, which uses numerical integration to approximate the nonlinear state posterior distribution, and avoids to calculate the Jacobian matrix associated with EKF directly. In addition, the authors have proposed some new update rules of weights for Gaussian sum filters, which improves the performance of filter significantly.

However, the uncertainty of noise covariance limited filters' application in the field of target tracking. To obtain accurate location estimation for maneuvering target, some researchers tried to update the noise covariance during the process of estimation and proposed adaptive EKF algorithms [19-21]. In order to overcome the uncertainty of noise covariance, Ge *et al.* proposed an adaptive UKF where the process noise covariance

The manuscript submitted on April 03, 2020, revised on June 11, 2020, accepted on July 20, 2020. This research work is supported by Natural Science Foundation of China (No. 61633008, No. 51609046), Natural Science Foundation of Heilongjiang Province under Grant F2015035, and China Scholarship Council (CSC) under Grant 201906680024.

Changjian Lin, Hongjian Wang (Corresponding author), Mingyu Fu, and Jianya Yuan are with the College of Automation, Harbin Engineering University, Harbin, 150001, China (e-mail: m18243088393@163.com, cctime99@163.com, fumingyu@hrbeu.edu.cn, 2414450031@qq.com).

Jason Gu is with the Department of Electrical and Computer Engineering, Dalhousie University, Halifax, NS, Canada (e-mail: Jason.gu@dal.ca).

is estimated by the innovation and residual sequences, and redundant measurement difference sequences are applied to resolve the measurement noise covariance in real time [22].

Arasaratnam *et al.* [23] pointed out the UKF existing problem of low precision or even divergence in solving the high-dimensional nonlinear state estimation problem by theoretical analysis and simulation experiments. Then they introduced the third-order spherical radial rule to approximate the state posterior distribution, and proposed Cubature Kalman Filter (CKF). In order to solve the reduction of numerical stability in CKF and improve filtering accuracy, the authors designed a square root CKF algorithm, which guarantees the positive definiteness and symmetry of the covariance matrix by passing the square root of the covariance matrix in the calculation process. Due to the convenience of CKF parameters selection and high filtering accuracy, it has been applied to state estimation problems in many fields [24-28]. In order to obtain higher accuracy of the numerical integration and estimation, the arbitrary degree spherical-radial rule-based High-degree CKF has been proposed and applied to the target state estimation [29, 30]. But this filter is not applicable to time-delay and non-Gaussian system. To solve this problem, the out-of-order sigma-point Kalman filter [31] and out-of-sequence particle filter [32] have been proposed based on the backward prediction and forward prediction, and the randomly delayed high-degree Cubature Huber-based Filtering has been proposed in which the system model is re-written by the Bernoulli random variables to describe the randomly delayed measurements [33].

Particle filters have been widely used because they can solve the state estimation problem for nonlinear non-Gaussian systems [34-40]. However, the degeneracy problem occurs after multiple iterations of particle filter [41]. Gitakawa [42] proposed a resampling technique to solve this problem. But after multiple sampling, the particle diversity will be destroyed, resulting in a sample impoverishment. Fu *et al.* [43] improved the resampling technique and proposed exquisite resampling. The improvements of particle flow filters have provided a promising avenue for the problem of weight degeneracy. Li *et al.* proposed numerous particle flow filters that calculate and update the weights of the particles by invertible mapping [44]. Nurminen *et al.* [45] introduced flow transformation into approximate Bayesian filtering for nonlinear and Gaussian state-space models whose measurement function is differentiable, where the random variable posterior-distributed is transformed by the prior-distributed one by Gaussian flow. In order to improve the real-time performance of particle filtering, Biswas *et al.* [46] reduced processing time of conventional particle filter combined with the extrapolated single propagation technique, where only one sample state vector is propagated per iteration. To tackle the sample degeneracy and the impoverishment, [47] suggests a self-evaluation method to track the posterior distribution and detect the low-weight particles.

As a highly nonlinear system, UUV has very complicated dynamic characteristics. As the most widely used equipment for underwater detection, sonar detection is sensitive to environmental noise and has a high false alarm rate. The uncertainty of UUV dynamics and the difficulty of underwater detection are the main challenges of UUV state estimation. In this paper, a gated recurrent units-based particle filter (GRUPF) for UUV state estimation is proposed. Gated recurrent units (GRU) can be used to fit systems with complex and uncertain mapping between input and output. Moreover, GRU has the characteristics of fast learning speed and strong generalization ability. Applying GRU to learn the dynamics model of UUV and fit the mapping between the previous measurements and the current target states can effectively improve the stability and accuracy of state prediction.

II. Related Work

In recent years, deep learning technology has been widely used to solve the problem of visual tracking. Among them, the deep learning model, which is mainly based on the convolutional neural network, is used to detect, identify and classify objects [48-50]. In addition, deep learning techniques have been used to improve the performance of filters. In [51], a deep neural network is used to further optimize the estimation result of KF. And it results in an enhancement in estimating the attitude states at near hover for the unmanned aerial vehicle. To solve the problem of that maneuvering movements cannot be timely modeled by pre-defined multiple models, Liu *et al.* [52] built a bidirectional long short-term memory-based deep learning maneuvering target-tracking algorithm for civil aircraft tracking. The neural network can quickly track maneuvering targets according to the target states once it has been fully trained. In order to change the input data with observation space into the target state space, the UKF algorithm with the transition matrix in the constant velocity shape is used to filter the azimuth and distance data in [52]. For nonlinear target tracking, Gao *et al.* [53] proposed long short-term memory-based recurrent neural networks to take in the observations and sequentially output the true states. This method acquires a higher accuracy than traditional methods in the problem of state estimation for a system with an explicit state transition equation and a single target state.

Although many filtering algorithms and related improved algorithms have been proposed, it is still challenging to obtain accurate state estimates due to the complexity and strong coupling of UUV dynamics and the inaccuracy of sonar measurements. The major contributions of our work are: 1) We designed a gated recurrent units-based particle filter based on deep learning technology, which can filter non-gaussian noise for nonlinear systems, 2) The proposed algorithm is successfully applied to the problem of UUV state estimation, which overcomes the problems of low accuracy and unstable estimation caused by the uncertainty of underwater measurement and the complexity of UUV dynamics, 3) Even in the case of short-term target loss, GRUPF can still achieve low error and stable target state estimation.

III. Problem Statement

The aim of nonlinear filtering task this paper address is to estimate the states of a system at time *k* according to a sequence

of observations collected up to time step *k*. The process model and measurement model are described as following:

$$\mathbf{X}_k^t = f_k\left(\mathbf{X}_{k-1}^t\right) + \omega_k \tag{1}$$

$$\mathbf{O}_k = g_k\left(\mathbf{X}_k, \upsilon_k\right) \tag{2}$$

Here $\mathbf{X}_k^t = \left[x_k^t, y_k^t, \dot{x}_k^t, \dot{y}_k^t\right]^T \in \mathbb{R}^m$ donates the target states at time step k, $\mathbf{X}_k^o = \left[x_k^o, y_k^o, \dot{x}_k^o, \dot{y}_k^o\right]^T \in \mathbb{R}^m$ represents observer states. Defined $\mathbf{X}_k = \left[x_k, y_k, \dot{x}_k, \dot{y}_k\right]^T \in \mathbb{R}^m$ as a relative states vector. Let $\mathbf{X}_k = \mathbf{X}_k^t - \mathbf{X}_k^o$. $f_k : \mathbb{R}^m \times \mathbb{R}^{m'} \to \mathbb{R}^m$ denotes state-transition function, $\mathbf{O}_k \in \mathbb{R}^n$ presents measurement of $\mathbf{X}_k$ measured by g_k: $\mathbb{R}^n \times \mathbb{R}^{n'} \to \mathbb{R}^n$ a nonlinear measurement model, $\omega_k \in \mathbb{R}^{m'}$ and $\upsilon_k \in \mathbb{R}^{n'}$ are process noise and measurement noise respectively, and they are not correlated to each other in this models.

A. System Model of UUV

The depth adjustment strategy of UUV often leads to greater pitch adjustment, which is not only negative to the attitude control of the target vehicle, but also affects the stability of the sensors. Therefore, the fixed-depth navigation mode is the primary choice for UUV cruise. In this section, a horizontal three degree of freedom control model is defined, which ignores the ship dynamics associated with heave, roll, and pitch motion. The global and body coordinates are shown in Fig. 1. Where the global coordinates are represented by the North East reference frame (*NOE*), $x_B o_B y_B$ is the reference frame of UUV which origin at centroid of UUV. The three degree of freedom control model of UUV is described below:

$$\dot{\eta} = \mathbf{R}(\psi)\mathbf{V} \tag{3}$$

$$\left(\mathbf{M}_{RB} + \mathbf{M}_A\right)\dot{\mathbf{V}} + \left(\mathbf{C}_{RB}(\mathbf{V}) + \mathbf{C}_A(\mathbf{V})\right)\mathbf{V} + \mathbf{D}(\mathbf{V})\mathbf{V} = \tau \tag{4}$$

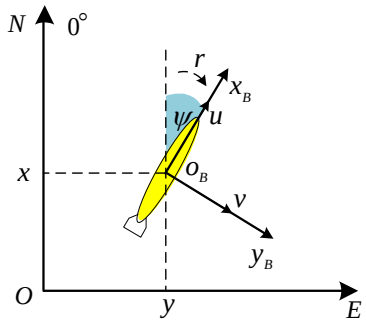

Fig. 1. The global and body coordinate system. The position and heading of UUV are described by global coordinate, and its velocity and yaw are described by body coordinate.

Where, $\boldsymbol{\eta} = [x, y, \psi]^T$ including position vector and heading of UUV in global coordinate system; $\mathbf{V} = [u, v, r]^T$ represents velocity vector corresponding to the surge, sway, and yaw of UUV in local coordinate system; $\mathbf{R}(\psi)$ is the transformation matrix from global coordinate system to local coordinate system; $\mathbf{M}_{RB}$ and $\mathbf{M}_A$ denote the inertia matrixes of rigid body and added mass respectively; $\mathbf{C}_{RB}$ and $\mathbf{C}_A$ are Coriolis-centripetal matrixes of rigid body and added mass respectively; $\mathbf{D}$ signifies the hydrodynamic damping matrix; and $\tau = [\tau_u \ 0 \ \tau_r]$ is the expression of actuator input. Specifically,

$$\mathbf{R}(\psi) = \begin{bmatrix} \cos\psi & -\sin\psi & 0 \\ \sin\psi & \cos\psi & 0 \\ 0 & 0 & 1 \end{bmatrix} \tag{5}$$

$$\mathbf{M} = \mathbf{M}_{RB} + \mathbf{M}_A = \begin{bmatrix} m - X_{\dot{u}} & 0 & 0 \\ 0 & m - Y_{\dot{v}} & mx_G - Y_{\dot{r}} \\ 0 & mx_G - Y_{\dot{r}} & I_z - N_{\dot{r}} \end{bmatrix} \tag{6}$$

$$\mathbf{C}(\mathbf{V}) = \mathbf{C}_{RB}(\mathbf{V}) + \mathbf{C}_A(\mathbf{V}) = \begin{bmatrix} 0 & 0 & Y_v v + Y_r r - m(x_G r + v) \\ 0 & 0 & mu - X_{\dot{u}} u \\ m(x_G r + v) - Y_v v - Y_r r & X_{\dot{u}} u - mu & 0 \end{bmatrix} \tag{7}$$

$$\mathbf{D}(\mathbf{V}) = \begin{bmatrix} X_{|u|u}|u| + X_u & 0 & 0 \\ 0 & Y_{|v|v}|v| + Y_v & -Y_{|v|r}|v| - Y_r \\ 0 & -N_{|r|v}|r| - N_v & N_{|r|r}|r| + N_r \end{bmatrix} \tag{8}$$

Then, the kinematic and dynamic equations of the UUV:

$$\begin{cases} \dot{u} = (-d_{11}u + \tau_u)/m_{11} \\ \dot{v} = (Am_{33} - Bm_{23})/(m_{22}m_{33} - m_{23}^2) \\ \dot{r} = (Bm_{22} - Am_{23})/(m_{22}m_{33} - m_{23}^2) \\ \dot{x} = u\cos(\psi) - v\sin(\psi) \\ \dot{y} = u\sin(\psi) + v\cos(\psi) \\ \dot{\psi} = r \end{cases} \tag{9}$$

where $A = -d_{22}v + (d_{23} - uc_{23})r$, $B = (d_{32} - uc_{32})v - d_{33}r + \tau_r$.

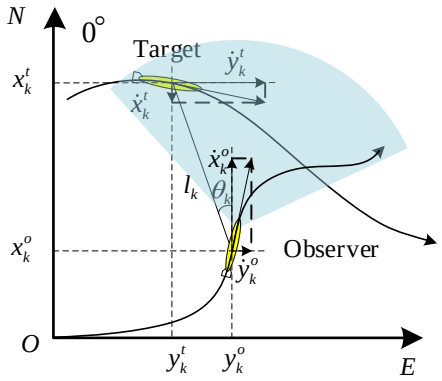

Fig. 2. The motion of observer and target in the global coordinate system. Once a target is detected by the observer, its motion relative to the observer will be obtained, including range, bearing, velocity, and course.

B. Measurement Model

We introduce UUV state estimation problem, which is to estimate the states of UUV using sonar measurements. The relative motion between observer and target is shown in Fig. 2. The measurement model is represented as:

This article has been accepted for publication in a future issue of this journal, but has not been fully edited. Content may change prior to final publication. Citation information: DOI 10.1109/TIM.2020.3011789, IEEE Transactions on Instrumentation and Measurement

$$\mathbf{O}_k = \begin{bmatrix} l_k \\ \theta_k \\ v_k \\ \beta_k \end{bmatrix} = \begin{bmatrix} \sqrt{y_k^2 + x_k^2} \\ \arctan\left(\frac{y_k}{x_k}\right) \\ \sqrt{\dot{y}_k^2 + \dot{x}_k^2} \\ \arctan\left(\frac{\dot{y}_k}{\dot{x}_k}\right) \end{bmatrix} + \upsilon_k \tag{10}$$

Where l_k, θ_k, v_k, β_k signify relative range, bearing, velocity, and course respectively.

IV. Gated Recurrent Units-Based Particle Filter

UUV state estimation involves nonlinear systems, non-Gaussian noise, large and complex environments, complex dynamics that are difficult to describe, and uncertain measurement. The basic idea of particle filtering is to use a set of samples to approximate the posterior probability of the system, and then use this approximate representation to estimate the state of the nonlinear system. There are a large number of samples required to approximate the posterior probability density of the system. The more complex the environment, the more samples are needed to describe the posterior probability and the higher the complexity of the algorithm. And the resampling will lead to the loss of sample validity and diversity, leading to sample depletion. Moreover, the uncertainty of underwater measurement reduces the estimation accuracy of the particle filter algorithm.

Aiming at the complex dynamics of UUV and the uncertainty of underwater measurement, a GRU-based deep neural network framework is established to predict the UUV states based on previous measurements. The chronological unfolding neural network framework based on GRU is shown in Fig. 3. As the figure shows, the GRU-based deep neural network framework consists of input layer, hidden layer, middle layer and output layer.

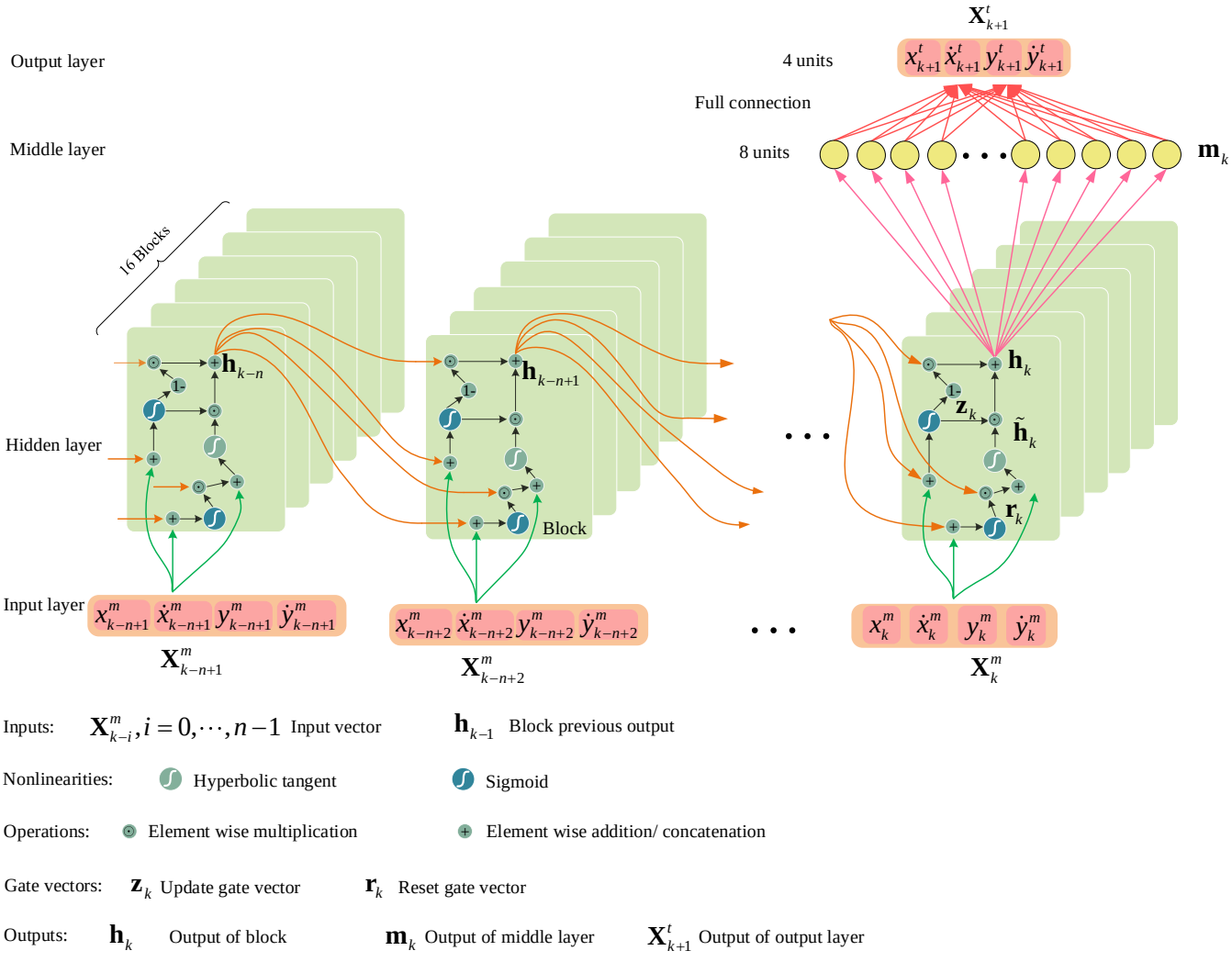

Fig. 3. The network structure of GRU based deep neural network framework unfold in time steps. (Bias units are omitted to simplify the visualization network.)

For the hidden layer, each GRU consists of a reset gate and an update gate. The reset gate can combine new information with the memory and help capture short-term information in the time series. The update gate determines the amount of memory information saved to the current moment, which can help the GRU capture long-term dependencies. Therefore, the GRU can

capture features in the time-dependent measured information, modeling the mapping between the previous measurements of the target and the current states of the target.

For this GRU-based deep neural network framework, the inputs are the measured states of target $\mathbf{X}_k^m$ at previous timesteps., the outputs are the UUV states vectors $\mathbf{X}_{k+1}^t$. The hidden layer consists of GRUs and fully connects with the middle layer. At each time step $k+1$, the target UUV measured states $\mathbf{X}_k^m$ at k time step are input to the network, and the useful features stored in the hidden layer which were captured from the historical states $\mathbf{X}_{0:k-1}^m$ are used for this prediction. At the same time, the features about $\mathbf{X}_k^t$ will be stored for subsequent predictions. Specifically:

$$\mathbf{z}_k = \sigma\left(\mathbf{W}_{hz}\mathbf{h}_{k-1} + \mathbf{W}_{oz}\mathbf{X}_k^m + \mathbf{b}_z\right) \tag{11}$$

$$\mathbf{r}_k = \sigma\left(\mathbf{W}_{hr}\mathbf{h}_{k-1} + \mathbf{W}_{or}\mathbf{X}_k^m + \mathbf{b}_r\right) \tag{12}$$

$$\tilde{\mathbf{h}}_k = \tanh(\mathbf{r}_k * (\mathbf{W}_{hh}\mathbf{h}_{k-1}) + \mathbf{W}_{oh}\mathbf{X}_k^m + \mathbf{b}_h) \tag{13}$$

$$\mathbf{h}_k = (1-\mathbf{z}_k) * \mathbf{h}_{k-1} + \mathbf{z}_k * \tilde{\mathbf{h}}_k \tag{14}$$

$$\mathbf{m}_k = \tanh\left(\mathbf{W}_{hm}\mathbf{h}_k + \mathbf{b}_m\right) \tag{15}$$

$$\mathbf{X}_{k+1}^t = \tanh\left(\mathbf{W}_{mx}\mathbf{m}_k + \mathbf{b}_x\right) \tag{16}$$

Where $\mathbf{r}_k$, $\mathbf{z}_k$, $\mathbf{h}_k$, $\mathbf{m}_k$ and $\mathbf{X}_{k+1}^t$ are output vectors of reset gate, update gate, hidden layer, middle layer and output layer respectively; $\mathbf{W}_{hz}$ and $\mathbf{W}_{hr}$ are the weight matrices from hidden states at previous time step to update gate and reset gate respectively; $\mathbf{W}_{oz}$, $\mathbf{W}_{or}$ and $\mathbf{W}_{oh}$ are the weight matrices from input vector $\mathbf{W}_k^m$ to update gate, reset gate and $\tilde{\mathbf{h}}_k$ respectively; $\mathbf{W}_{hh}$ is the weight matrices from hidden states at previous time step to $\tilde{\mathbf{h}}_k$; $*$ denotes element wise multiplication. When $\mathbf{r}_k \approx 0$, the hidden states are ignored and only the current input is used to reset the hidden states. This operation can help the current input forget the useless information for the future. $\mathbf{W}_{hm}$ and $\mathbf{W}_{mx}$ are fully connected weight matrices referring to hidden layer, middle layer and output layer; $\sigma(\cdot)$ and $\tanh(\cdot)$ are sigmoid and hyperbolic tangent functions; in all of the above formulas, $\mathbf{b}$ are bias.

The optimal number of hidden and middle layer neurons and the parameters are determined by experiments. Typically, the larger the number of samples in the dataset, the more neurons are needed for the hidden and middle layer. To improve the optimization efficiency, train the model across a small data set containing only half of the data of the full dataset firstly, and determine the optimal number of hidden and middle layer neurons for this small data. Then, grow the number of hidden and middle layer neurons by a factor of about 2, and the model was then trained across the full data set to further determine the number of neurons in the hidden and middle layer.

The UUV target state estimation process based on GRUPF is as follows:

1. Calculating all the measured states from estimation step $k-1$ to k of target UUV $\mathbf{X}_{k-1:k}^m$ according to the measurement $\mathbf{O}_{k-1:k}$ and states of observer $\mathbf{X}_{k-1:k}^o$.

$$\mathbf{X}_{k-1:k}^m = \begin{bmatrix} l_{k-1:k}\cos\left(\theta_{k-1:k}\right) \\ l_{k-1:k}\sin\left(\theta_{k-1:k}\right) \\ v_{k-1:k}\cos\left(\beta_{k-1:k}\right) \\ v_{k-1:k}\sin\left(\beta_{k-1:k}\right) \end{bmatrix} + \mathbf{X}_{k-1:k}^o \tag{17}$$

2. Sampling particles $\{\mathbf{X}_k^{m(i)}\}_{i=1}^N$ from measured state set. For UUV target state estimation, the detection frequency of the sensor is much higher than the frequency of state estimation, so it is feasible to sample particles from the measured data. And the sampling particles distributed in $p\left(\mathbf{X}_k^m\right)$.

3. Pre-trained GRU-based deep neural network is used to predict the state of sampled particles.

$$\mathbf{X}_{k+1}^{t(i)} = \mathrm{GRU}\left(\mathbf{X}_k^{m(i)}\right) \tag{18}$$

Where $\mathrm{GRU}(\cdot)$ represents the deep neural network.

4. Estimating UUV states according to the follows:

$$\begin{aligned} E[\mathrm{GRU}\left(\mathbf{X}_k^m\right)] &= \int \mathrm{GRU}\left(\mathbf{X}_k^m\right) p(\mathbf{X}_k^m) d\mathbf{X}_k^m \\ &= \frac{1}{N}\sum_{i=1}^N \mathrm{GRU}\left(\mathbf{X}_k^{m(i)}\right) \end{aligned} \tag{19}$$

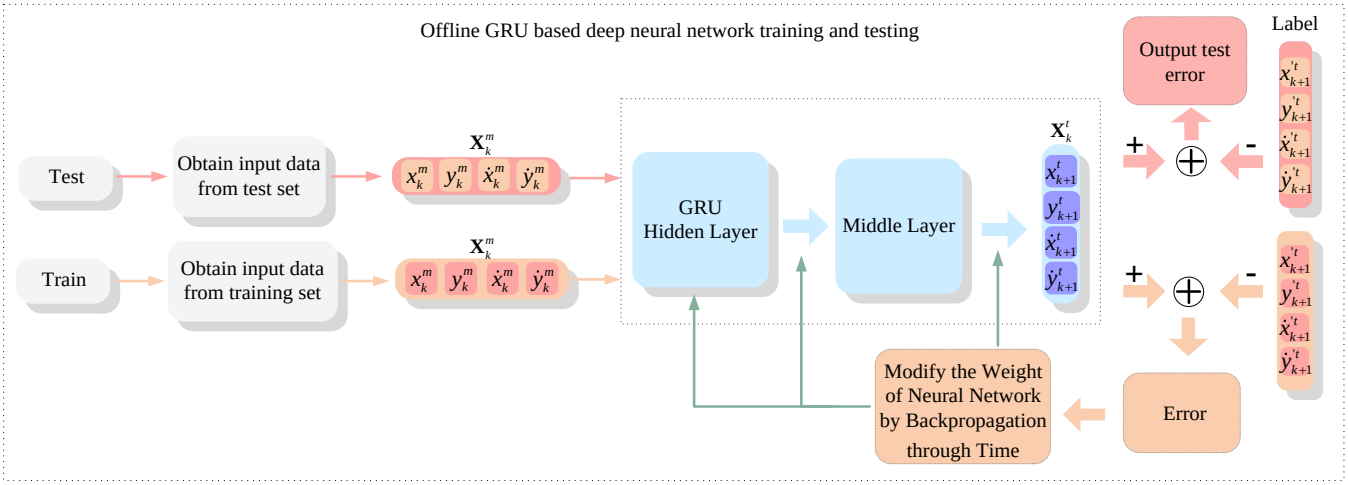

Fig. 4. The training of GRU based deep neural network framework.

V. Construction of GRUPF for Target UUV State Estimation

The training process of GRU based deep neural network framework is shown in Fig. 4. The network framework is trained offline, and the fully trained network will be used to predict the states including position and velocity of the target UUV online according to the measured states at previous timesteps.

The network framework contains 4 input units and 4 output units correspond to the measured states at previous timesteps and the predicted target states respectively. The dataset consists of 8×10^5 training samples, 8×10^4 validation samples and 500 test samples. Each sample contains a set of input and a label corresponding to the measured states at previous timesteps and the real states of the estimated target. In the process of training, minibatch gradient descent through time and Adam optimizer are applied to minimize mean squared error loss function, the initial learning rate is set to 10^{-2} with 10^{-6} decay, and the batch size is set as 10^4. Fig. 5 shows the loss of the deep neural network on train and validation sets. The loss on the train and validation sets have similar convergence trends. In early stage of training, the network converges rapidly. The speed of convergence gradually decreases until it converges to a close vicinity to zero with iteration. Taking learning ability, exploration ability and generalization ability of the network into consideration, the loss is expected to converge to an error close to zero, not zero, so that the estimator can deal with the problem of state estimation in low SNR environment.

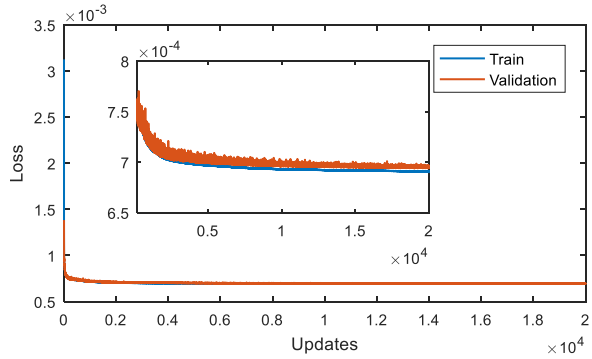

Fig. 5. The mean squared error of the deep neural network.

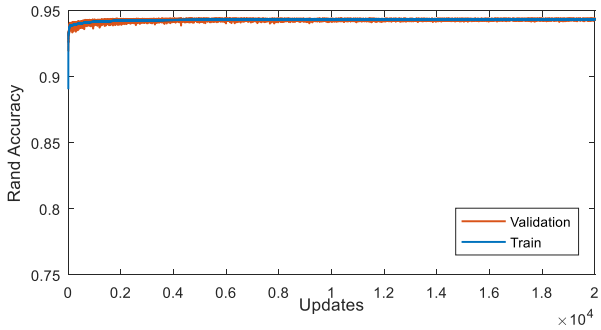

Fig. 6. The Rand accuracy of the deep neural network.

Fig. 6 shows the Rand accuracy [54] of the deep neural network on train and validation sets. It can be seen from the network Rand accuracy curve that the convergent network has higher Rand accuracy on both the train and validation sets.

VI. Simulations and Analysis

To test the performance of the GRUPF for UUV state estimator, statistical experiment and illustrative example are given in this section. For each $\boldsymbol{\upsilon}$ in measurement $\mathbf{O}$, its measurement noises are modeled as Gaussian noise with a mean of $\mathbf{u}$ and a variance of $\mathbf{R}_n$, and its expression is

$$p(\boldsymbol{\upsilon}) = N(\boldsymbol{\upsilon}; \mathbf{u}, \mathbf{R}_n) \tag{20}$$

A. Statistical Experiment

In order to verify the performance of state estimator under different noises, a statistical experiment is designed in this section. The experiment counted the localization root mean square error (RMSE) of different methods on 105 Monte Carlo runs with different observation noises, respectively. For every Monte Carlo run, the motion state of target is one of the constant velocity motions (first 35 runs), constant acceleration motion (middle 35 runs) and constant turning motion (last 35 runs). Three sets of experiments were conducted under different noise environments. In the three sets of experiments, $\mathbf{R}_n$ is set as:

$$\begin{bmatrix} 1\,\mathrm{m}^2 & 0.01\,\mathrm{rad}^2 & 0.1\,\mathrm{m}^2/\mathrm{s}^2 & 0.001\,\mathrm{rad}^2/\mathrm{s}^2 \end{bmatrix},$$
$$\begin{bmatrix} 2\,\mathrm{m}^2 & 0.02\,\mathrm{rad}^2 & 0.2\,\mathrm{m}^2/\mathrm{s}^2 & 0.002\,\mathrm{rad}^2/\mathrm{s}^2 \end{bmatrix},$$
$$\begin{bmatrix} 4\mathrm{m}^2 & 0.04\,\mathrm{rad}^2 & 0.4\,\mathrm{m}^2/\mathrm{s}^2 & 0.004\,\mathrm{rad}^2/\mathrm{s}^2 \end{bmatrix}.$$

And set $\mathbf{u} = \begin{bmatrix} 0 & 0 & 0 & 0 \end{bmatrix}$. The performance of KF, EKF, UKF ($\kappa = 3-n$), CKF, PF (500 particles), and GRUPF (50 particles) based state estimator in the three sets of experiments are shown in Table 1. The localization RMSE is defined as

$$RMSE_p = \sqrt{\frac{1}{m}\sum_{k=1}^{m}\left(x_i^k - \hat{x}_i\right)^2 + \left(y_i^k - \hat{y}_i\right)^2} \tag{21}$$

Where m is the number of Monte Carlo runs, x_i^k, y_i^k denote the kth estimated north and east position of target UUV in time step i, $\hat{x}_i, \hat{y}_i$ represent the real north and east position of target UUV in time step i. And the RMSE of velocity is defined as

$$RMSE_v = \sqrt{\frac{1}{m}\sum_{k=1}^{m}\left(\dot{x}_i^k - \dot{\hat{x}}_i\right)^2 + \left(\dot{y}_i^k - \dot{\hat{y}}_i\right)^2} \tag{22}$$

Where $\dot{x}_i^k, \dot{y}_i^k$ denote the estimated north and east velocity of target UUV, $\dot{\hat{x}}_i, \dot{\hat{y}}_i$ represent the real north and east velocity of target UUV in time step i.

As shown in Table 1, the localization RMSE increases with the increase of the covariance of observation noise, and the stability of each target estimation method decreases with the increase of the covariance of observation noise. KF gets the poorest performance in all three sets of experiments. EKF obtain good stability and RMSE at the first set of experiment, but it is sensitive to measurement noise. UKF, CKF, and PF

show good stability and accuracy in the first and second sets of experiments. But, in the third set, CKF and PF show poor stability. UKF and GRUPF based state estimation methods are insensitive to the measurement noise compared with other methods. Under the influence of the same observation noise, GRUPF always acquires the minimum localization RMSE and shows stronger stability.

TABLE I. LOCALIZATION AND VELOCITY RMSE OF THE SIX STATE ESTIMATION METHODS.

Set	Algorithm	Lowest Localization RMSE (m)	Highest Localization RMSE (m)	Median Localization RMSE (m)	Average Localization RMSE (m)	Lowest Velocity RMSE (kn)	Highest Velocity RMSE (kn)	Median Velocity RMSE (kn)	Average Velocity RMSE (kn)
Set 1	KF	3.0887	13.3567	3.6337	5.2297	0.4366	1.2014	0.6771	0.7822
	EKF	0.9731	3.3937	1.2488	1.455	0.1507	1.2377	0.2568	0.3328
	UKF	0.7434	6.0252	1.8395	2.1389	0.0332	0.2997	0.1195	0.1225
	CKF	0.7384	9.7522	1.2996	2.1066	0.1229	0.4322	0.1991	0.2084
	PF	0.6857	3.3944	1.4748	1.6089	0.04846	0.2784	0.089	0.0984
	GRUPF	0.19474	1.848	0.3583	0.4837	0.0086	0.1498	0.0351	0.0911
Set 2	KF	3.1.46	18.3436	3.6464	5.3184	0.4408	1.2048	0.7066	0.8119
	EKF	1.3282	5.8642	3.3364	3.2166	0.0698	2.6774	0.4431	0.7634
	UKF	0.8985	7.2477	2.0713	2.4447	0.0351	0.2645	0.1275	0.1324
	CKF	0.9528	9.2232	2.3972	3.2182	0.142	0.517	0.2734	0.2856
	PF	0.5247	7.6604	1.9736	2.1915	0.0575	0.2558	0.1141	0.1196
	GRUPF	0.2949	1.356	0.5668	0.5957	0.0111	0.1143	0.0245	0.0722
Set 3	KF	3.0755	15.3458	3.6558	5.2985	0.4715	1.2082	0.7484	0.8421
	EKF	3.3787	9.8048	4.8991	5.3144	0.3795	1.8578	0.8826	0.9722
	UKF	1.0108	10.2136	2.4266	2.8095	0.0351	0.286	0.1474	0.1489
	CKF	1.4182	10.7522	3.4748	4.1848	0.1811	0.4877	0.2843	0.287
	PF	1.2822	16.6442	2.473	3.0135	0.0441	0.3684	0.1177	0.1437
	GRUPF	0.3452	1.344	0.6416	0.6626	0.0137	0.1744	0.0377	0.103

For velocity RMSE, KF gets the poorest stability in all three sets of experiments. The stability and accuracy of EKF decrease with the increase of the covariance of measurement noise. In the view of the change of the covariance of measurement noise, UKF, CKF, PF, and GRUPF show good stability and accuracy in all three sets of experiments.

It can be seen from Table 1 that GRUPF has high accuracy and strong stability in tracking constant velocity, constant acceleration, and constant turning target. GRUPF is insensitive to measurement noise both in low-order position estimation and high-order velocity estimation, which makes it very suitable for underwater target state estimation.

B. Illustrative Examples

This section will further test the performance of GRUPF-based state estimation method through illustrative examples. The trajectories of observer and target are shown in Fig. 7. Assuming that the maximum velocity of the observer is 3 kn, and that of target UUV is 6 kn, the observer sonar measures a 120° sector coverage area with 120 m circumference radius. The variance of measurement noise is set to $[1\mathrm{m}^2 \quad 0.01\mathrm{rad}^2 \quad 0.1\mathrm{m}^2/\mathrm{s}^2 \quad 0.001\mathrm{rad}^2/\mathrm{s}^2]$. The detection frequency of the sonar is set to 50 Hz, the estimation frequency is set to 1 Hz, the number of particles is set as 50. The number of Monte Carlo simulations is set to 100 for each illustrative example.

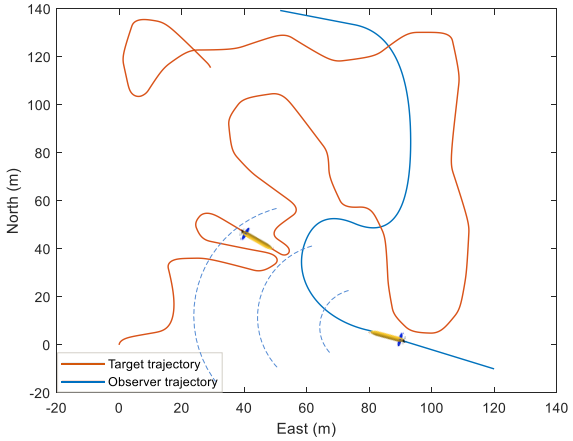

Fig. 7. The trajectories of target UUV and observer.

In order to analyze the performance of GRUPF, this section compares it with Gaussian mixture unscented Kalman filter (GM-UKF) [55] and Gaussian mixture cubature Kalman filter (GM-CKF) [56]. For GM-UKF and GM-CKF, the Singer model is used to build the process model of UUV. Fig. 8 shows the estimated trajectories of GM-UKF, GM-CKF and GRUPF

based state estimation methods for target UUV in scenario 1. In this scenario, the observer navigates at a constant velocity, and the target UUV is far away from the observer. In this case, the movement of UUV is complex and changeable. It can be clearly seen from the estimated trajectory of Fig. 8 that GRUPF has the best estimation performance in this scenario.

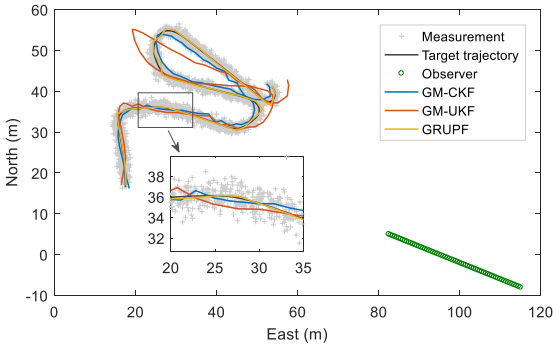

Fig. 8. The estimated trajectories of various methods in scenario 1.

Fig. 9 and Fig. 10 show the localization RMSE in east and north of the three methods respectively. As can be seen from the Figures, GM-UKF based state estimation method obtains the lowest estimation accuracy both in east and north position, and the maximum localization RMSE in north is more than 5m. Compared with GM-UKF, the localization RMSE of GM-CKF is more stable, and the east and north localization RMSE are roughly distributed within 0-2 m. As can be seen from Fig. 9 and Fig. 10, compared with the other two methods, the GRUPF based state estimation method not only obtains the lowest localization RMSE, but also the most stable localization RMSE. Even if the target UUV suddenly changes its state of motion, the estimation performance of GRUPF is only slightly affected, and it can still estimate the position of the target with high accuracy.

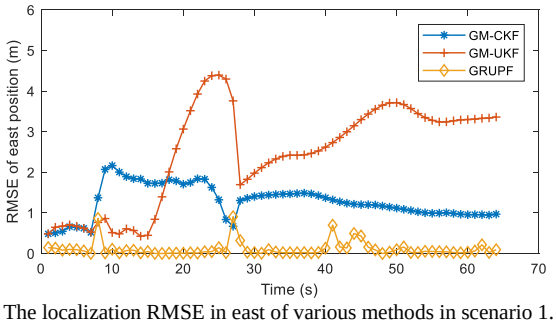

Fig. 9. The localization RMSE in east of various methods in scenario 1.

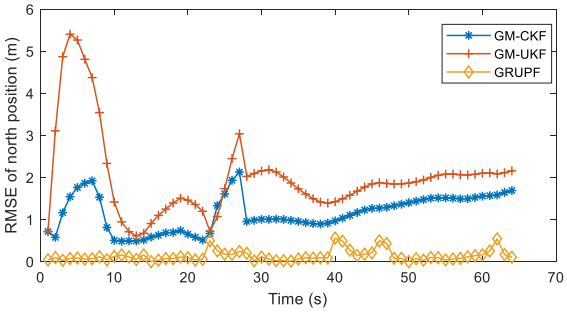

Fig. 10. The localization RMSE in north of various methods in scenario 1.

Fig. 11 and Fig. 12 show the RMSE of east and north velocity of the three methods respectively. The trend of velocity RMSE curves of GM-UKF and GM-CKF is similar, and the RMSE is poor when the target's state of motion is changing. As opposed to localization RMSE, GM-UKF gets lower velocity RMSE than GM-CKF. As with the localization RMSE curve, GRUPF achieves the lowest RMSE and the best stability.

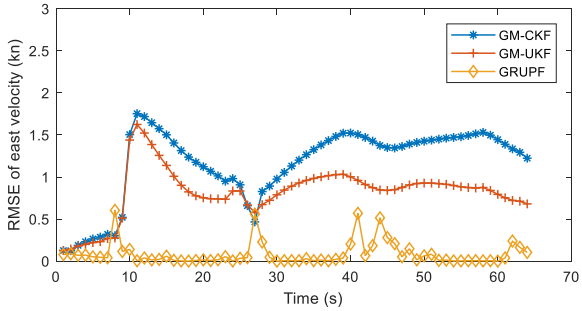

Fig. 11. The velocity RMSE in east of various methods in scenario 1.

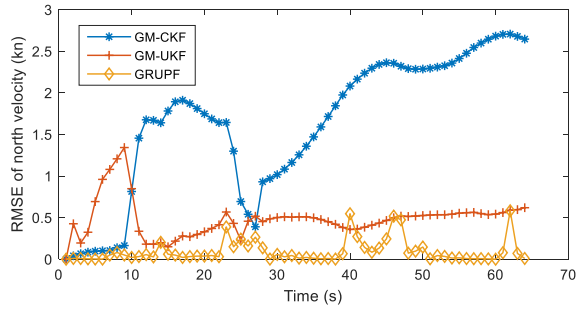

Fig. 12 The velocity RMSE in north of various methods in scenario 1.

Fig. 13 shows the estimated trajectories of GM-UKF, GM-CKF and GRUPF based state estimation methods for target UUV in scenario 2. In which, the observer navigates with a constant turn rate. In this case, the motion mode of the target UUV is simpler than that in scenario 1, and the motion mode of the observer is more complex than that in scenario 1. It can be seen from the estimated trajectories that GRUPF performs best, followed by GM-CKF, and GM-UKF gets the poorest estimation trajectory.

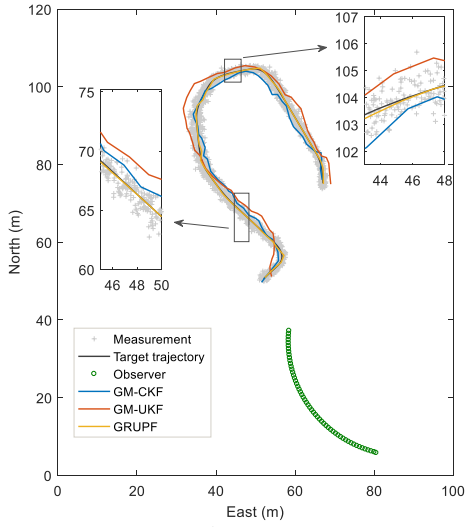

Fig. 13. The estimated trajectories of various methods in scenario 2.

Fig. 14-17 show the localization and velocity RMSE of the three methods in scenario 2 respectively. Same as scenario 1, compared with GM-UKF and GM-CKF, GRUPF achieves the minimum RMSE both in localization and velocity. Moreover, compared with GM-UKF, GM-CKF obtains lower localization RMSE. And the velocity estimate of GM-UKF is better than GM-CKF. Obviously, the RMSE of localization and velocity in this scenario is more stable than that in scenario 1. This indicates that the motion model of the target has a strong influence on the accuracy of the target state estimation. And compared with GM-UKF and GM-CKF, the accuracy of state estimation of GRUPF is the least affected by target motion state.

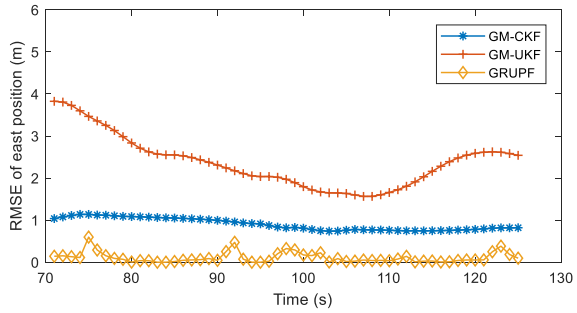

Fig. 14. The localization RMSE in east of various methods in scenario 2.

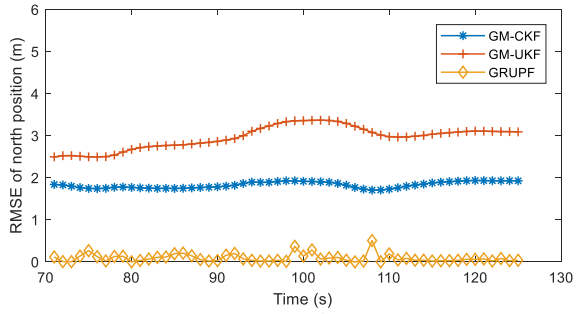

Fig. 15. The localization RMSE in north of various methods in scenario 2.

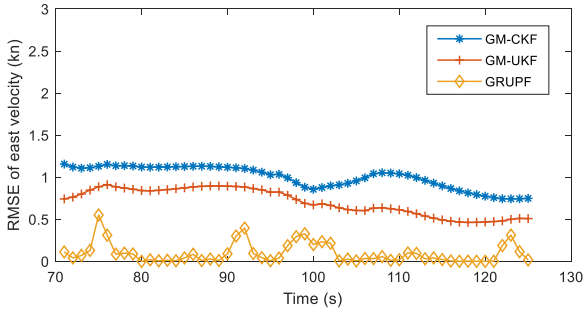

Fig. 16. The velocity RMSE in east of various methods in scenario 2.

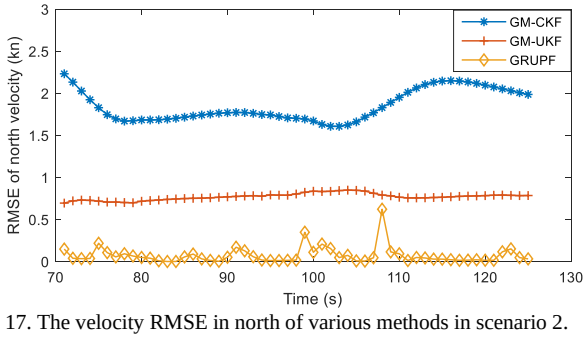

Fig. 17. The velocity RMSE in north of various methods in scenario 2.

Fig. 18 shows the estimated target UUV trajectories of GRUPF in scenario 3. In which, the observer navigates with variable accelerations. In this scenario, the target is lost for a short time as the observer and the target UUV navigate. In the case of target loss, sampling cannot be performed from the measurement data. At this time, the outputs of the network at the previous moment are used as the inputs of the current moment.

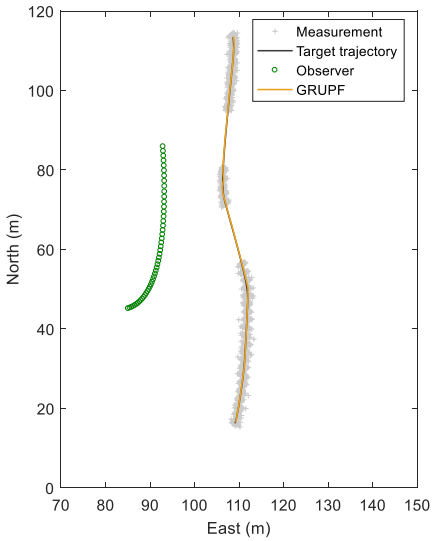

Fig. 18. The estimated trajectory of GRUPF in scenario 3.

The curves of east and north localization RMSE are shown in Fig. 19 and Fig. 20The curves east and north velocity RMSE are shown in Fig. 21 and Fig. 22. In this scenario, the north state of motion of target UUV is more stable than that in eastward, therefore, the estimation for the north target states is more accurate and more stable. The localization and velocity RMSE curves are basically distributed around 0, and the target loss has little effect on the accuracy of GRUPF state estimation. Even if the target suddenly changes its state of motion, the localization and velocity RMSE of the GRUPF are affected little, with only slight fluctuations.

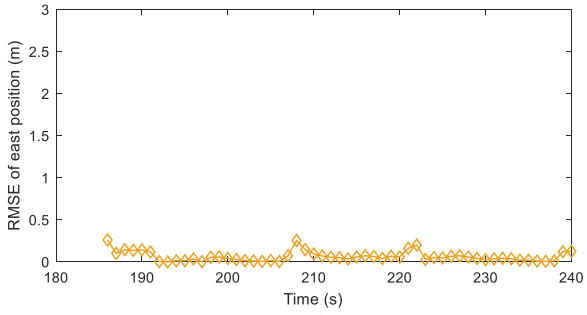

Fig. 19. The localization RMSE in east of GRUPF in scenario 3.

As can be seen from the above illustrative examples, the GRUPF-based state estimation method obtains the smallest localization RMSE in all examples, followed by GM-CKF. It also achieves the best performance in velocity estimation. And the estimation accuracies of position and velocity of GM-CKF and GM-UKF are seriously affected by the changes in target

state of motion of. On the contrary, the accuracy of state estimation of GRUPF is slightly affected by the changes in motion state of target. Simulation results in scenario 3 show that GRUPF can achieve accurate target state estimation even when the target is temporarily lost.

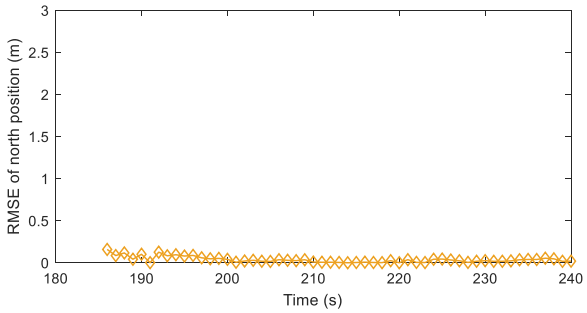

Fig. 20. The localization RMSE in north of GRUPF in scenario 3.

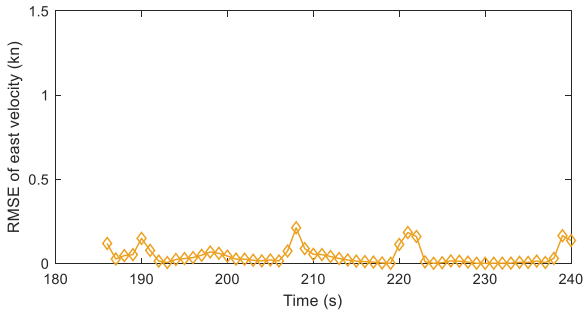

Fig. 21. The velocity RMSE in east of GRUPF in scenario 3.

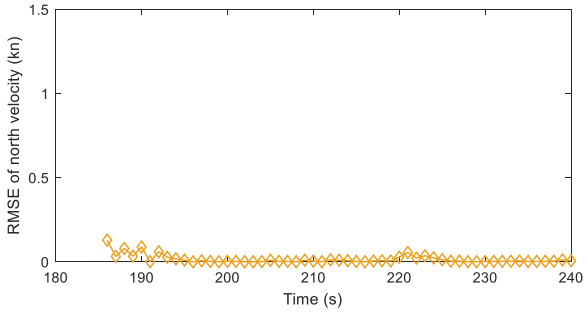

Fig. 22. The velocity RMSE in north of GRUPF in scenario 3.

VII. Conclusion

In order to solve the problems of low accuracy and unstable estimation of the UUV target states caused by the uncertainty of underwater measurement and the complexity of UUV dynamics, a GRU-based particle filter is proposed in this paper. A deep neural network framework is established based on GRUs to learn the mapping between the measured states at previous timesteps and current states of target. Thanks to the strong ability of learning and generalization of GRU, the network can learn the dynamics model of UUV and recognizes the measurement noise. Therefore, the proposed filter can deal with the uncertainty in UUV state estimation caused by the complexity of UUV dynamic and the nonlinearity of UUV system. The filter samples directly from the previous measurement data and approximates the distribution of measurement with these particles. Then fully trained the deep neural network is used to predict the current states of sampling particles, so that GRUPF can identify and filter the non-linear and uncertain measurement noise. In order to investigate the performance of the proposed GRUPF, the performance of state estimators based on KF, EKF, UKF, CKF, PF, and GRUPF are counted under three different noise intensities. The statistics show that the GRUPF is insensitive to noise in both low-order position estimation and high-order velocity estimation. It is stable under all the three groups of noise interference. To further test the performance of the proposed GRUPF, the estimation performance is compared with the GM-UKF and GM-CKF based state estimation methods in different scenarios. The proposed GRUPF is found to be superior to the other two methods in both accuracy and stability. Even in the case of short-term target loss, GRUPF can still achieve low error and stable target state estimation.

References

[1] T. B. Santoso, E. Widjiati, Wirawan and G. Hendrantoro, "The Evaluation of Probe Signals for Impulse Response Measurements in Shallow Water Environment," *IEEE Transactions on Instrumentation and Measurement*, vol. 65, no. 6, pp. 1292-1299, June 2016.

[2] T. Matsuda, T Maki, T Sakamaki, T Ura, "State Estimation and Compression Method for the Navigation of Multiple Autonomous Underwater Vehicles with Limited Communication Traffic," *IEEE Journal of Oceanic Engineering*, vol 40, no. 2, pp. 337-348, Apr. 2015.

[3] J. C. Kinsey, Q. Yang, J. C. Howland, "Nonlinear Dynamic Model-Based State Estimators for Underwater Navigation of Remotely Operated Vehicles," *IEEE Transactions on Control Systems Technology*, vol.22, no. 5, pp. 1845-1854, Sept. 2014, 10.1109/TCST.2013.2293958

[4] G. Fagogenis, D. Flynn, D. M. Lane, "Improving Underwater Vehicle navigation state estimation using Locally Weighted Projection Regression," *2014 IEEE International Conference on Robotics and Automation (ICRA)*, Hong Kong, China, 31 May-7 June 2014.

[5] J. Cui and Z. Li, "Synchronous Three-Dimensional Imaging and Velocity Estimation of Underwater Targets Using Pulse-Pair Acoustical Imaging Technique," *IEEE Transactions on Instrumentation and Measurement (Early Access)*, DOI: *10.1109 / TIM.2019.2957912*

[6] K. Shojaei, M. Dolatshahi, "Line-of-sight target tracking control of underactuated autonomous underwater vehicles," *Ocean Engineering*, vol. 133, pp. 244-252, Mar. 2017.

[7] M. N. Santhosh1, S. K. Rao, R. P. Das, and K. L. Raju, "Underwater Target Tracking using Unscented Kalman Filter," *Indian Journal of Science and Technology*, vol. 8, no. 31, Nov. 2015.

[8] Y. Zhang, L. Gao, "Sensor-Networked Underwater Target Tracking Based on Grubbs Criterion and Improved Particle Filter Algorithm," *IEEE Access*, vol. 7, pp. 142894-142906, Sept. 2019.

[9] J. K. Lee, "A Parallel Attitude-Heading Kalman Filter Without State-Augmentation of Model-Based Disturbance Components," *IEEE Transactions on Instrumentation and Measurement*, vol. 68, no. 7, pp. 2668-2670, July 2019.

[10] D. Simon, "Optimal State Estimation: Kalman H Infinity and Nonlinear Approaches," USA, NJ, Hoboken:Wiley, 2006.

[11] H. Mohammadi, Y. Hong, G. Khademi, et al. "Extended Kalman filtering for state estimation of a Hill muscle model," *IET Control Theory & Applications*, vol. 12, no. 3, pp. 384-394, Jan. 2018.

[12] M. Masoumnezhad, A. Jamali and N. Nariman-Zadeh, "Robust gmdh-type neural network with unscented Kalman filter for nonlinear systems," *Transactions of the Institute of Measurement and Control*, vol.38, no. 8, pp. 1–12, 2016.

[13] S. Julier, J. Uhlmann, and H. Durrant-Whyte, "A new method for the nonlinear transformation of means and covariances in filters and estimators," *IEEE Transactions on Automatic Control*, vol. 45, no. 3, pp. 477–482, Mar. 2000.

[14] S. J. Julier and J. K. Uhlmann, "Unscented filtering and nonlinear estimation," in *Proceedings of the IEEE*, vol. 92, no. 3, pp. 401-422, Ma. 2004.

[15] N. Xia, M. Weitnauer, "TDOA-Based Mobile Localization Using Particle Filter With Multiple Motion and Channel Models," *IEEE Access*, vol. 7, pp. 21057-21066, Feb. 2019.
[16] W.Yi, L. Fu, Á. Fernández, L. Xu, and L. Kong, "Particle filtering based track-before-detect method for passive array sonar systems," Signal Processing, vol. 165, pp. 303-314, 2019.
[17] C. Liu, B. Li and W. Chen, "Particle Filtering with Soft State Constraints for Target Tracking," *IEEE Transactions on Aerospace and Electronic Systems*, vol. 55, no. 6, pp. 3492-3504, Dec. 2019.
[18] K. Ito, K. Xiong, "Gaussian filters for nonlinear filtering problems," *IEEE Transactions on Automatic Control*, vol. 45, no. 5, pp. 910-927, May 2000.
[19] G. Kumar, D. Prasad, "Singh, R.P. Target tracking using adaptive Kalman Filter," in *Proceedings of the 2017 International Conference on Smart grids, Power and Advanced Control Engineering, Bangalore*, India,17–19 Aug. 2017, pp. 376–380.
[20] V. Lippiello, B. Siciliano, L. Villani, "Visual motion tracking with full adaptive extended Kalman filter: An experimental study," in *Proceedings of the 16th IFAC World Congress*, Prague, Czech Republic, 3–8 July 2005; pp. 283–288.
[21] M. Ghobadi, P. Singla and E. T. Esfahani, "Robust Attitude Estimation from Uncertain Observations of Inertial Sensors Using Covariance Inflated Multiplicative Extended Kalman Filter," *IEEE Transactions on Instrumentation and Measurement*, vol. 67, no. 1, pp. 209-217, Jan. 2018.
[22] B. Ge, H. Zhang, L. Jiang, Z. Li, and M. Butt, "Adaptive Unscented Kalman Filter for Target Tracking with Unknown Time-Varying Noise Covariance," *Sensors*, vol. 19, no. 6, Mar. 2019.
[23] I. Arasaratnam, S. Haykin, "Cubature Kalman Filters," *IEEE Transactions on Automatic Control*, vol. 54, no. 6, pp. 1254-1269, May 2009.
[24] F. Ma, J. He, X. and Zhang, "Robust Kalman Filter Algorithm Based on Generalized Correntropy for Ultra-Wideband Ranging in Industrial Environment," *IEEE Access*, vol.7, pp. 27490-27500, Feb. 2019.
[25] A. Zhang, S. Bao, F. Gao, W. Bi, "novel strong tracking cubature Kalman filter and its application in maneuvering target tracking," *Chinese Journal of Aeronautics*, vol. 32, no. 11, pp. 2489-2502, 2019.
[26] S. Jie, Q. Guoqing, L. Yinya and S. Andong, "Stochastic convergence analysis of cubature Kalman filter with intermittent observations," J*ournal of Systems Engineering and Electronics*, vol. 29, no. 4, pp. 823-833, Aug. 2018.
[27] R. He, S. Chen, H. Wu, Z. Liu, J. Chen, "Optimal Maneuver Strategy of Observer for Bearing-Only Tracking in Threat Environment," *INTERNATIONAL JOURNAL OF AEROSPACE ENGINEERING*, vol. 2018, id. 7901917, pp. 1-9, Jul. 2018.
[28] H. Feng, Z. Cai, "Target tracking based on improved cubature particle filter in UWSNs," *IET Radar Sonar and Navigation*, vol. 13, no. 4, pp. 638-645, 2019.
[29] B. Jia, M. Xin and Y. Cheng, "High-degree cubature Kalman filter," *Automatica*, vol. 49, no. 2, pp. 510–518, 2013.
[30] H. Liu and W. Wu, "Interacting multiple model (IMM) fifthdegree spherical simplex-radial cubature Kalman filter for maneuvering target tracking," *Sensors*, vol. 17, no. 6, pp. 1–12, 2017.
[31] G. L. Plett, D. Zarzhitsky and D. J. Pack, "Out-of-order sigma-point Kalman filtering for target localization using cooperating unmanned aerial vehicles," *Advances in Cooperative Control and Optimization*, 21–43, 2007.
[32] Y. Kim, K. Hong and H. Bang, "Utilizing out-of-sequence measurement for ambiguous update in particle filtering," I*EEE Transactions on Aerospace & Electronic Systems*, vol. 54, no. 1, pp. 493–501, Aug. 2017.
[33] W.Qin, X. Wang, N. Cui, "Robust filtering with randomly delayed measurements and its application to ballistic target tracking in boost phase," *Transactions of the Institute of Measurement and Control*, vol. 41, no. 7, pp. 2077–2088, 2019.
[34] H. X. Li, T. B. Schon, and L. Ljung, "A basic convergence result for particle filtering," *IEEE Transactions on Signal Processing*, vol. 56, no. 4, pp. 1337–1348, Apr. 2008.
[35] S. Hu, L. Shi, Y. Zha, M. Williams, L. Lin, "Simultaneous state-parameter estimation supports the evaluation of data assimilation performance and measurement design for soil-water-atmosphere-plant system," *Journal of Hydrology*, vol. 555, pp. 812–831, 2017.
[36] F. Cheng, L. Qu, W. Qiao, L. Hao, "Enhanced Particle Filtering for Bearing Remaining Useful Life Prediction of Wind Turbine Drivetrain Gearboxes," *IEEE Transactions on Industrial Electronics*, vol. 66, no. 6, pp. 4738-4748, Aug. 2019.
[37] I. Kyriakides, D. Morrell, and A. Papandreou-Suppappola, "Sequential Monte Carlo methods for tracking multiple targets with deterministic and stochastic constraints," *IEEE Transactions on Signal Processing*, vol. 56, no. 3, pp. 937–948, Mar. 2008.
[38] S. Perez-Vieites, I. Marino, J. Miguez, "Probabilistic scheme for joint parameter estimation and state prediction in complex dynamical systems," *Physical Review E*, vol. 98, no. 6, Dec. 2018.
[39] W. Meeussen, J. Rutgeerts, K. Gadeyne, H. Bruyninckx, and J. De Schutter, "Contact-state segmentation using particle filters for programming by human demonstration in compliant-motion tasks," *IEEE Transactions on Robotics*, vol. 23, no. 2, pp. 218–231, Apr. 2007.
[40] C. Wen-Yan, C. Chu-Song, and J. Yong-Dian, "Visual tracking in highdimensional state space by appearance-guided particle filtering," *IEEE Transactions on Image Processing*, vol. 17, no. 7, pp. 1154–1167, Jul. 2008.
[41] A. Doucet, S. Godsill, C. Andrieu, "On sequential Monte Carlo sampling methods for Bayesian filtering," *Statistics and Computing*, vol. 10, no. 3, pp. 197-208, 2000.
[42] K. Gitakawa, "Monte Carlo filter and smoother for non-Gaussian state space models," *Journal of Computational and Graphical Statistics*, vol. 5, no. 1, pp. 1-25, 1996.
[43] X. Fu, Y. Jia, "An Improvement on Resampling Algorithm of Particle Filters," *IEEE Transactions on Signal Processing*, vol. 58, no. 10, pp. 5414-5420, Jun.2010.
[44] Y. Li, M. Coates, "Particle Filtering with Invertible Particle Flow," *IEEE Transactions on Signal Processing*, vol. 65, no. 15, pp. 4102–4116, 2017.
[45] H. Nurminen, R. Piché and S. Godsill, "Gaussian flow sigma point filter for nonlinear Gaussian state-space models," in *2017 20th International Conference on Information Fusion (Fusion)*, Xi'an, 2017, pp. 1-8.
[46] S. K. Biswas, A. G. Dempster, "Approximating Sample State Vectors using the ESPT for Computationally Efficient Particle Filtering," *IEEE Transactions on Signal Processing*, vol. 67, no. 7, pp. 1918-1928, Feb. 2019.
[47] M. Ahwiadi and W. Wang, "An Adaptive Particle Filter Technique for System State Estimation and Prognosis," *IEEE Transactions on Instrumentation and Measurement (Early Access)*, DOI: 10.1109 / TIM.2020.2973850.
[48] F. Bi, M. Lei, Y. Wang, "Context-aware MDNet fortarget tracking in UAV remote sensing videos," *International Journal of Remote Sensing*, vol.41, no.10, pp. 3784-3797, Jan 2020.
[49] S. Cai, J. Liang, Q. Gao, C. Xu and R. Wei, "Particle Image Velocimetry Based on a Deep Learning Motion Estimator," *IEEE Transactions on Instrumentation and Measurement (Early Access)*, DOI: 10.1109 / TIM.2019.2932649.
[50] T. Zhang, S. Liu, X. He, H. Huang, and K. Hao, "Underwater Target Tracking Using Forward-Looking Sonar for Autonomous Underwater Vehicles," *Sensors*, vol. 20, no. 1, 102, Jan. 2020.
[51] M. K. Al-Sharman, Y. Zweiri, M. A. K. Jaradat, R. Al-Husari, D. Gan and L. D. Seneviratne, "Deep-Learning-Based Neural Network Training for State Estimation Enhancement: Application to Attitude Estimation," *IEEE Transactions on Instrumentation and Measurement*, vol. 69, no. 1, pp. 24-34, Jan. 2020.
[52] J. Liu, Z. Wang, M. Xu, "DeepMTT: A deep learning maneuvering target-tracking algorithm based on bidirectional LSTM network," *Information Fusion*, vol.53, pp. 289-304, Jan. 2020.
[53] C. Gao, J. Yan, S. Zhou, B. Chen, H. Liu, "Long short-term memory-based recurrent neural networks for nonlinear target tracking," *Signal Processing*, vol. 164, pp. 67-73, Nov. 2019.
[54] W. M. Rand, "Objective criteria for the evaluation of clustering methods," *Journal of the American Statistical Association*, vol.66, no. 336, pp. 846–850, 1971.
[55] F. Faubel, J. Mcdonough, D. Klakow, "The Split and Merge Unscented Gaussian Mixture Filter," *IEEE Signal Processing Letters*, vol. 16, no. 9, pp. 786-791, Jun. 2009.
[56] C. Li, "Research on State Estimation and Control Method of Target Tracking of Sea Surface Rescue," Ph.D. dissertation, Dept. Automat., Harbin Engineering University, Harbin, China, 2018.

Changjian Lin received the B. S. degree from the electrical engineering and automation, Changchun University of Science and Technology, China, in 2015. She is currently pursuing the Ph. D. degree in control science and engineering, Harbin Engineering University, China.

Her current research interests include navigation and control, intelligent control methods, machine learning, deep learning, and state estimation.

Hongjian Wang was born in Harbin, Heilongjiang Province, China in 1971. She received the B.S. and M.S. degrees in computer science from the Heilongjiang University in 1993 and Harbin Engineering University in 1998, and the Ph.D. degree in control theory and control engineering from Harbin Engineering University in 2004.

From 1993 to 1998, she was a Research Assistant working in Harbin Engineering University, from 1998 to 2003, she was a Lecturer, and from 2003 to 2005 she was an Associate Professor. Since 2005, she has been a Professor with the Automation College and was a doctoral tutor from 2006. During 2004 to 2006, she worked in the post-doctoral mobile station of Harbin Institute of Technology. She is the author of one book, more than 100 articles, and more than 30 inventions. Her research interests include autonomy control and swarm intelligence for unmanned systems, intelligent optimization theory and methods, machine learning, deep learning, deep reinforcement learning, target tracking, simultaneous localization and mapping (SLAM), etc.

Prof. Wang was a recipient of the Young Academic Elite of Heilongjiang Province in 2008 and been funded by the National Science Foundation and the Ministry of education's doctoral program special research fund. She is a peer reviewer of Journal of automation, Control theory and application, Robot, and Journal of Harbin Engineering University, etc. and holds 14 patents. She is the corresponding author of this article.

Mingyu Fu received the Ph.D. degree from the College of Automation, Harbin Engineering University, Harbin, China, in 2005. She is currently a Professor and the Ph.D. Supervisor with Harbin Engineering University.

Her current research interests include vessel dynamic positioning control, automatic control of unmanned surface vehicle, and hovercraft motion control.

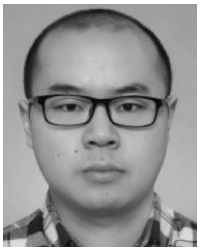

Jianya Yuan received the B. S. degree from the electrical engineering and automation, Mudanjiang Normal University, China. He is currently pursuing the Ph. D. degree in control science and engineering, Harbin Engineering University, China.

His current research interests include multi-agent, path planning, and Deep Q-learnings.

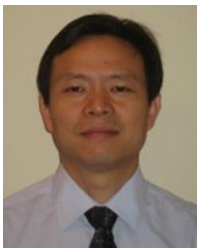

Jason Gu Jason Gu (SM'06) received the bachelor's degree in electrical engineering and information science from the University of Science and Technology of China, Hefei, China, in 1992, the master's degree in biomedical engineering from Shanghai Jiaotong University Shanghai, China, in 1995, and the Ph.D. degree in electrical and computer engineering from the University of Alberta, Edmonton, AB, Canada, in 2001. He is currently a Full Professor of electrical and computer engineering with Dalhousie University, Halifax, NS, Canada. He is also a Cross-Appointed Professor with the School of Biomedical Engineering for his multidisciplinary research work.

He has authored or co-authored more than 300 journals, book chapters, and conference papers. His current research interests include biomedical engineering, biosignal processing, rehabilitation engineering, neural networks, robotics, mechatronics, and control. Dr. Gu is the IEEE member of SMC and RAS. He is a fellow of Engineering Institute of Canada and Canada Academy of Engineering. He is currently the IEEE Canada President-Elect from 2018 to 2019. He has been an Editor for Journal of Control and Intelligent Systems, Transactions on Canadian Society for Mechanical Engineering, the IEEE Transactions on Mechatronics, IEEE SMC Magazine, International Journal of Robotics and Automation, and the IEEE Access.